Journal of Liquid Chromatography and Gas Chromatography, Europe
https://technicalreport.org/lcgceu/

LC GC Eu., Vol. 39, No.1, 07-15, 2026

Technical Reports Press

REVIEW ARTICLE

Relaxation-Time and Uncertainty Atlas for Electrochemical Impedance Spectroscopy in Molecular and Bioelectronic Junctions

Peter W. Carr[1*] **and Robert Freeman**[1]

[1]*Professor of Chemistry, University of Minnesota*
[2]*Department of Chemistry, Faculty of Science, Sakarya Applied Sciences University, Sakarya, Türkiye*
[*]*Corresponding author*

Corresponding author:
petecarr@umn.edu

Received: 10 September 2025
Accepted: 19 December 2025
Available online: 30 March 2026

Abstract

Despite resolving a rich set of molecular and bioelectronic phenomena such as charge transport, polarization, dielectric effects, and interfacial dynamics, EIS suffers from ambiguity and lack of identifiability that allows the assignment of any arbitrary circuit to molecular impedance characteristics. In this work we introduce a relaxation-time atlas with identifiability criteria and uncertainty quantification procedures for discerning molecular effects from contact resistance, pad and fringe capacitance, ionic screening, dipolar polarization, geometry effects, instrument response, and other non-molecular parasitic effects that could swamp the intrinsic molecular behavior. Our atlas uses a physically explicit impedance decomposition, frequency scaling tests specific to a mechanism, Kramers–Kronig consistency, identifiability checks, and rules for uncertainty quantification. The credibility of each assigned molecular impedance parameter is quantified in the form of a Molecular Impedance Credibility Index (MICI). Rather than taking an equivalent circuit label as evidence of molecular behavior, MICI provides a measure of support for the assignment of each component and its value to molecular effects. We develop the validation logic specifically for self-assembled monolayer tunnel junctions, molecular wire junctions, ion-containing devices, solvent sensitive devices, protein junctions, mesoscopic quantum RC circuits, and atomic contacts. The proposed methodology thus represents a protocol for consistent analysis of molecular junction impedances based on geometric, frequency response, temperature, and voltage conditions as well as environmental manipulations, parasitic corrections, and uncertainty quantification procedures.

Keywords: electrochemical impedance spectroscopy; molecular electronics; molecular junctions; bioelectronics; relaxation time; admittance; parasitic capacitance; contact resistance; Kramers–Kronig validation; uncertainty analysis

1. Introduction

Molecular electronics relies on the use of single-molecule constructs, self-assembled monolayers, molecular films, proteins, and related assemblies as functional electronic elements. The problem is not just detecting low currents flowing through nanometer-scale junctions, but the separation of the molecular behavior from contacts, electrodes, dielectrics, mobile ions, molecular orientation, mechanics, and other measurement artifacts [1–4]. Molecular devices are not ideal two-terminal conductors, but hybrid electronic devices with electronic coupling, molecular packing, interface order, electrode surface roughness, oxidation, solvent dipoles, mobile ions, and other effects contributing to the measured response [1–4].

The conventional methodology has been built on the analysis of static current-voltage measurements and the tunneling expression

$$J = J_0(V)\exp(-\beta d), \tag{1}$$

where J is current density, $J_0(V)$ is a voltage-dependent prefactor, β is the tunneling decay constant, and d is molecular wire length or film thickness [5]. While equation (1) applies to short, nonconducting and

Cite as: P. W. Carr & R. Freeman (2026). Relaxation-Time and Uncertainty Atlas for Electrochemical Impedance Spectroscopy in Molecular and Bioelectronic Junctions. LC GC Eu., 39(1) (2026) 07-15.

weakly dispersive barriers, many molecular devices operate far beyond the narrow regime where it is valid. Longer wires, redox-active films, proteins, mixed-ionic-electronic devices may have mechanisms based on hopping, polaronic transport, dielectric relaxation, injection barriers, electric-field screening, and/or structure modification in response to bias [6–8]. A static J-V measurement merges all these processes into one and fails to reveal their differences, which are critical for the mechanism assignment and device operation.

EIS overcomes this limitation by measuring the complex impedance $Z(\omega)$

$$Z(\omega) = Z'(\omega) + iZ''(\omega), \tag{2}$$

or the admittance $Y(\omega) = 1/Z(\omega)$ over a range of angular frequencies $\omega = 2\pi f$. In molecular junctions, EIS allows separating resistance and capacitance contributions, quantifying dielectric behavior, detecting ionic dynamics, distinguishing between contact and molecular limitations, and comparing the results with other types of measurements [9–12]. This strength, however, leads to an interpretation difficulty since several circuits can produce similar Nyquist plots and Bode diagrams; also, constant phase elements can represent various sources of disorder while intrinsic molecular capacitance may be comparable to parasitic capacitance [13–16].

The question, then, becomes quite specific: under what experimental conditions a certain EIS parameter can be interpreted as a molecular one? The requirement to show the agreement with data alone is insufficient since a molecular interpretation is meaningful only when the same parameter exhibits the scaling and behavior associated with the proposed mechanism. At the same time, the distinction between the molecular contribution and various sources of interference becomes especially important as the field transitions from conceptual studies to quantitative comparison among junction designs.

This paper provides four concrete contributions. First, it introduces a framework for the decomposition of measured impedance into molecular, contact, parasitic, and ion/dipole contributions prior to assigning any circuit elements to the measured data. Second, it identifies the regimes of impedance relaxation along with corresponding scaling laws and frequency signatures. Third, it proposes a parameter-specific score known as the Molecular Impedance Credibility Index (MICI) for evaluating the evidentiary base supporting each molecular assignment. Fourth, it establishes a protocol for the validation of an assignment based on linearity, stability, Kramers-Kronig consistency, identifiability, geometry-related scaling, contact control, environmental perturbation, and the raw-data reporting.

2. Analytical scope and interpretive methodology

This study analyzes the state of the art in the molecular and bioelectronic impedance spectroscopy with an eye towards developing a general framework for systematic data interpretation. Heterogeneity in the spectral coverage, measurement details, model description, and data analysis code makes it imperative to formulate a common standard for reproducible interpretation before a fitted parameter is qualified as an intrinsic feature of the device studied. The goal of this research is to establish a data-driven process by which the measured impedance can be consistently analyzed and validated.

Included works fulfill one of the following criteria: (i) EIS or high-frequency admittance has been employed for the characterization of molecular, self-assembled, bioelectronic, atomic or mesoscopic junctions; (ii) the impedance data have been analyzed to extract contact, resistance, capacitance, dielectric, ionic or interface-related contributions; (iii) impedance behavior has been compared to that of J-V or temperature-dependent transport measurements, thickness scaling, contact effects, or environmental perturbation; or (iv) theoretical insights or analytical approaches useful for impedance analysis are provided. Studies dealing with electrochemical impedance or mesoscopic devices are included if they provide a validation protocol applicable to molecular impedance metrology.

It should be noted that the assignment of a measured impedance parameter as molecular is not enough for a molecular assignment to be made. Instead, an evaluation will be performed based on the parameter's ability to exhibit scaling or other expected features associated with the particular type of impedance relaxation while remaining distinct from contacts, parasitics, and environmental dispersion. Table 1 summarizes the minimum information needed for reproducible and scientifically rigorous analysis.

Table 1: Minimum information required for rigorous analysis of molecular-junction EIS studies.

Information class	Required or strongly recommended details
Device architecture	Bottom electrode, anchoring chemistry, molecular layer identity, top contact, junction area, thickness or molecular length, number of measured devices, fabrication yield.
Frequency-domain protocol	Frequency range, AC amplitude, DC bias, integration time or points per decade, instrument bandwidth, calibration procedure, open/short/load correction where relevant.
Validation status	Evidence of linearity, causality, stability, Kramers–Kronig consistency, repeated spectra, time-drift controls, bias-history controls.
Model specification	Equivalent circuit, fitted parameter values, confidence intervals, residuals, parameter covariance, alternative circuit tests, physical justification of each element.
Scaling tests	Area dependence, thickness or length dependence, temperature dependence, bias dependence, environmental perturbation, contact comparison.
Parasitic correction	Estimated lead resistance, pad capacitance, fringe capacitance, substrate leakage, instrument phase error, fixture contribution.
Mechanistic assignment	Explicit argument for classifying the dominant response as molecular, contact-limited, dipolar, ionic, quantum, or parasitic.
Reusability	Availability of raw impedance spectra, code, digitized data, device statistics, and fitting scripts.

3. The molecular EIS measurement problem

3.1. From measured impedance to physical impedance

The measured impedance of a molecular junction is rarely identical to the intrinsic impedance of the molecular layer. A minimal decomposition is

$$\begin{aligned} Z_{\text{meas}}(\omega,V,T,A,d) = Z_{\text{par}}(\omega,A,\mathscr{G}) + Z_{\text{contact}}(\omega,V,T,\Gamma) \\ + Z_{\text{mol}}(\omega,V,T,d) + Z_{\text{ion/dip}}(\omega,V,T,\mathscr{E}). \end{aligned} \tag{3}$$

where Z_{par} represents parasitic and geometric terms, Z_{contact} contact and lead terms, Z_{mol} the molecular or film response, and $Z_{\text{ion/dip}}$ ionic or dipolar environmental terms. The symbols A, d, V, and T denote junction area, molecular thickness, bias, and temperature. The variables $\mathscr{G}$, Γ, and $\mathscr{E}$ denote device geometry, electronic coupling or contact structure, and environmental state. Eq. (3) is not a unique circuit model; it is an accounting relation that identifies which contributions must be bounded or removed before a parameter can be assigned to molecular origin.

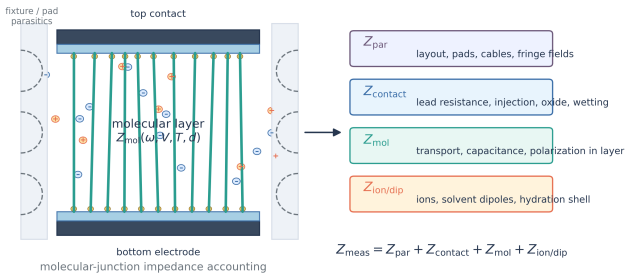

Figure 1: Impedance decomposition for a molecular or bioelectronic junction. The measured response contains molecular transport and polarization together with contact, ion/dipole, and parasitic contributions. The figure illustrates why parameter assignment requires geometry, contact, environmental, and fixture controls before an impedance element is identified as molecular.

Figure 1 summarizes the measurement hierarchy used throughout the article. The schematic emphasizes that a fitted circuit element becomes physically meaningful only after the molecular, contact, environmental, and geometric components have been bounded by independent controls.

For an ideal molecular monolayer treated as a parallel-plate dielectric, the capacitance is

$$C_{\mathrm{SAM}} = \frac{\varepsilon_0 \varepsilon_{\mathrm{r}} A_{\mathrm{geo}}}{d}, \tag{4}$$

where ε_0 is the vacuum permittivity, ε_{r} the apparent relative permittivity, A_{geo} the geometric area, and d the layer thickness. Eq. (4) is often used to infer ε_{r}. Its validity depends on whether the measured capacitance is dominated by the active molecular area rather than interfacial dipoles, electrode roughness, oxide layers, water or solvent uptake, fringe fields, or pad capacitance. The relation $C \propto A/d$ is therefore necessary for a molecular capacitance assignment but is not sufficient by itself.

A tunneling resistance assigned to the molecular layer should display length dependence of the form

$$RA = R_0 A \exp(\beta d), \tag{5}$$

where RA is the resistance–area product and $R_0 A$ is the extrapolated zero-length resistance–area contribution. If RA changes by orders of magnitude without a corresponding change in molecular length, packing, orbital structure, or electronic coupling, contact quality or device geometry is the more conservative explanation.

3.2. Why equivalent circuits are useful but insufficient

Equivalent circuits provide compact descriptions of frequency-dependent behavior. A common molecular-junction representation places a series contact resistance in series with a parallel molecular resistance and capacitance,

$$Z(\omega) = R_{\mathrm{c}} + \left(\frac{1}{R_{\mathrm{SAM}}} + i\omega C_{\mathrm{SAM}} \right)^{-1}. \tag{6}$$

The model can decouple a thickness independent resistance component from a molecular resistance component with an exponential increase with length and can evaluate molecular capacitance where geometries are well defined [9]. Eq. (6) is descriptive and cannot be interpreted until the validity of each element is individually verified. A series component attributed to contact resistance can incorporate contributions from leads, oxide, non-ohmic top contacts, or fixtures. A capacitance component associated with molecular layer can incorporate fringe capacitance as well as any contribution from pads. A molecular resistance element can incorporate injection barriers or interfacial tunneling.

The non-uniqueness of the equivalent circuit model is one of the core problems of impedance spectroscopy [13, 14]. Two entirely different circuit models can fit statistically indistinguishably over a certain frequency range. The inclusion of additional parameters can compensate for noise, drift, unmeasurable mechanisms, or other sources of errors. This is problematic in molecular junction studies since capacitance is relatively low, contact structure is hard to reproduce, and the available frequency window may not include all time constants involved. Quality of the fit must therefore be assessed together with perturbation experiments and the statistical uncertainty in the parameters.

3.3. Linearity, causality, stability, and Kramers–Kronig compliance

EIS analysis assumes a linear and causal response of the system to a perturbation around a stable equilibrium. If these criteria do not apply, it is possible to obtain a smoothly varying spectrum and residuals consistent with noise even in the presence of nonlinear or unstable processes. Kramers-Kronig checks validate linearity and causality as well as stationarity of the response [14, 17, 18]. Such validation is particularly important in molecular junctions due to potential bias induced structural changes, solvent absorption, ion migration, and electromigration.

Validation of Kramers–Kronig relations should be included as standard procedure in molecular EIS data reporting. While the lack of such validation does not necessarily invalidate the obtained spectrum, it makes claims based on the existence of a small imaginary part, use of CPE, or multiple overlapping time constants less valid. Tests for amplitude dependence, repeat experiments, and forward/reverse sweep measurements provide additional support to show that the data is collected in the stationary and small-signal regime.

3.4. Constant-phase element and the problem of apparent capacitance

The definition of constant phase element (CPE) is usually expressed as

$$Z_{\mathrm{CPE}}(\omega) = \frac{1}{Q(i\omega)^{\alpha}}, \qquad 0 < \alpha \leq 1, \tag{7}$$

where Q is a proportionality factor while α defines the deviation from a perfect capacitor. CPE model is useful in describing systems with non-ideal capacitive responses due to surface irregularities, a wide range of relaxation times, heterogeneous structures, or a broad relaxation path distribution [14, 15]. Parameter Q cannot be converted to an exact physical capacitance without further assumptions about the structure of resistors, interfaces, and topology.

This issue is fundamental in the context of molecular junctions where contact irregularities, defects, multiple conductive paths, or fringe fields will lead to an apparent low capacitance but in reality, Q will reflect the heterogeneity of the system. The CPE model itself should always be reported directly unless there is justification for using a conversion model. If such a conversion is performed, a thorough analysis of the residual should be provided and a comparison with at least one other reasonable model made.

4. Relaxation-Time Atlas for Molecular Impedance Spectroscopy

4.1. Need for relaxation-time approach in molecular EIS

Equivalent circuits provide a description of the impedance in terms of elements. In molecular junctions, there is a large distribution of microscopic environments in which individual molecules may differ with respect to tilt, bonding, proximity to defects and solvents, etc.

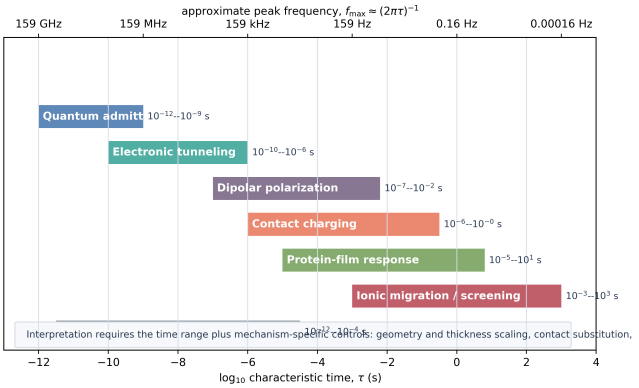

Figure 2: Relaxation-time atlas for molecular and bioelectronic EIS. The ranges indicate typical time-scale domains for quantum admittance, electronic tunneling, dipolar polarization, contact charging, protein-film response, ionic migration or screening, and geometric parasitics. Mechanism assignment requires the time scale plus the physical controls listed in Table 2.

The use of a distribution of relaxation times (DRT) to characterize impedance is a more natural approach in this case. The impedance can be written as

$$Z(\omega) = R_\infty + \int_{-\infty}^{+\infty} \frac{g(\ln\tau)}{1+i\omega\tau}\, d\ln\tau, \tag{8}$$

where R_∞ is high-frequency impedance, $g(\ln\tau)$ is a relaxation time distribution, and τ is a characteristic time. Solution of the inverse problem (retrieval of DRT) using equation (8) is ill-posed and needs some form of regularization [19, 20]. However, it allows determination of whether a circuit parameter represents a narrow relaxation, broad relaxation distribution, or an unresolved combination of multiple relaxation processes.

In the case of an ideal RC process, the characteristic relaxation time is

$$\tau = RC = \frac{1}{2\pi f_{\max}}, \tag{9}$$

where $f_{\max}$ is the frequency at which the semi-circle reaches its imaginary maxima in Debye-like manner. In molecular EIS, the same characteristic τ can originate from different processes such as charge relaxation, dipole rotation, ionic migration, charging of contacts, polarization in protein film, and pad capacitance. Table 2 provides classification of molecular impedance based on physical origin, impedance signature, validation experiment, and possible risks of misinterpretation.

Figure 2 places these regimes on a common time-axis scale. The diagram is intentionally interpreted with the validation criteria in Table 2, because a time constant alone cannot identify a mechanism in a nanoscale junction.

5. Evidence domains in molecular and bioelectronic EIS

Figure 3 illustrates the diagnostic separation required before parameters are assigned. The calculated signatures show how molecular, parasitic, and ionic contributions can generate visually similar impedance traces while responding differently to length, area, and parasitic controls.

5.1. SAM tunnel junctions

SAM junctions are crucial platforms for molecular EIS in that they enable thickness control and provide fairly well defined metal–molecule interfaces [9, 21, 22]. In the ideal case, impedance can be decomposed into molecular resistance, molecular capacitance, and contact or series

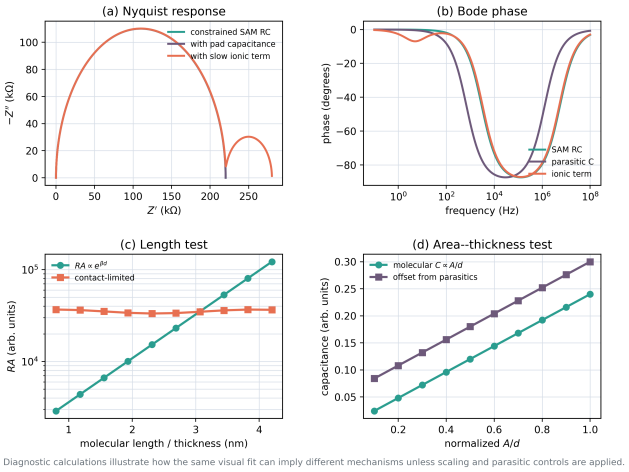

Figure 3: Diagnostic EIS signatures used to separate molecular response from parasitic and ionic contributions. (a) Nyquist traces for a constrained molecular RC response, the same response with additional pad capacitance, and a response containing a slow ionic term. (b) Corresponding Bode phase behavior. (c) Length dependence distinguishes exponential molecular tunneling from contact-limited resistance. (d) Area–thickness scaling separates molecular capacitance from capacitance with parasitic offset.

resistance. Length-dependent studies furnish clear evidence in that tunneling resistance scales exponentially with length, while capacitance should scale with thickness.

The most convincing SAM analysis combines RA scaling, $C \propto A/d$ scaling, and transport. Akkerman and colleagues relate the tunneling conductance through SAMs to a barrier model adjusted by image potential correction based on impedance and J–V data [23]. Sangeeth and colleagues analyze the molecular, surface, and contact contributions to the impedance separately, showing how EIS can assign molecular and contact effects with geometric constraints [9]. These studies illustrate the general validation scheme: circuit elements become meaningful when they are bounded simultaneously by length, area, and other transport measurements.

A critical caveat is inherent in SAM EIS because a compliant top contact, a layer with trapped charges, or non-covalent bonds in a liquid may yield contact-dominated impedance spectra. One molecular length and one junction geometry do not determine the origin of the fitted resistance. To assign a resistance uniquely, a series of molecular lengths and a series of junction designs with top-contact controls are required.

5.2. Conjugated wires and enhanced dielectric response

A new challenge arises with conjugated and donor–acceptor molecular wires because their polarizability and orbital hybridization, packing and ordering may significantly affect both conductivity and dielectric response. High capacitances reported for densely packed conjugated SAMs imply that collective electrostatic effects arise from molecular packing beyond bulk material expectations [11, 24]. Capacitance reflects, therefore, not only parasitic contributions, but also molecular organization, tilt angle, conjugation length, donor–acceptor structure, and electrostatics of the interfaces.

The enhancement of capacitance may also arise from geometric factors, surface defects, contaminants, trapped charges, oxide layers, leakage paths, or fringe fields. The claims of unusual dielectric properties require confirmation via length-dependence studies, active-area scaling, environmental comparison, solvent or humidity control, structural characterization, and polarizability prediction. Electronic structure theory provides the molecular polarizability, yet experimental validation through area scaling and contact control remains essential since the measured capacitance is a property of the entire junction [25, 26].

Table 2: Relaxation-time and uncertainty atlas for molecular and bioelectronic impedance. The categories are not mutually exclusive because a single device can contain several active contributions.

Regime	Likely physical origin	Expected impedance signature	Key validation test	Main risk
Electronic tunneling	Coherent or weakly dissipative transport through short molecular barriers	RA increases exponentially with d; capacitance approximately follows A/d; weak thermal activation	Length series; area scaling; comparison with J–V and barrier models	Contact resistance misidentified as molecular resistance
Hopping or polaronic transport	Multistep transport through localized states in longer molecules or redox-active films	Stronger temperature dependence; possible bias-dependent relaxation; deviation from simple tunneling decay	Temperature-dependent EIS; length-dependent activation energy; comparison with Marcus or hopping models	Static tunneling model forced onto activated transport
Contact-limited response	Injection barrier, oxide layer, soft top contact, contact reconfiguration, incomplete wetting	Thickness-independent or weakly thickness-dependent resistance; strong dependence on electrode chemistry or contact method	Contact substitution; zero-length extrapolation; independent contact controls	Apparent molecular resistance overestimated
Dipolar polarization	Molecular dipoles, interfacial dipoles, solvent orientation, donor–acceptor polarization	Capacitive or CPE-like dispersion; bias- and environment-sensitive phase response	Environment control; non-polar versus polar solvent comparison; dielectric scaling	Dipoles conflated with ionic migration
Ionic migration or screening	Mobile ions inside or near the molecular layer; field redistribution; ion-pair motion	Low- to mid-frequency capacitance increase; hysteresis; temperature-shifted roll-off; strong dependence on ionic content	Humidity and ion controls; temperature activation; bias-history tests; time-domain relaxation	Slow drift mistaken for stationary impedance
Bioelectronic film response	Protein polarizability, hydration shell, redox cofactors, interfacial electrostatics	Apparent protein capacitance and resistance; strong dependence on electrode–protein coupling	Length series; contact-engineered geometries; hydration and temperature controls	Interface dominates apparent protein conductivity
Quantum admittance	Phase-coherent mesoscopic conductor or atomic-scale contact	Admittance rather than classical impedance is primary; small or non-classical imaginary response	GHz calibration; comparison with quantum RC theory; channel-count control	Classical capacitance assigned to quantum density-of-states effects
Parasitic geometry	Pad capacitance, fringe fields, cables, substrate leakage, fixture inductance	Area- or layout-dependent capacitance not linked to the molecule; high-frequency artifacts	Open/short/load correction; blank devices; geometry simulation; fixture controls	Parasitic capacitance interpreted as molecular dielectric constant

5.3. Iono-electronic and solvent-sensitive junctions

Molecular junctions with solvents, mobile ions, or atmosphere-sensitive components allow for a translation of small changes in external parameters to large changes in conductance, capacitance, or rectification. EIS is perfectly adapted to these systems because dipolar polarization and ionic motion operate at distinct frequency ranges. Carbon-based molecular junctions exposed to acetonitrile vapor and mobile lithium ions reveal how internal electric fields can be reshaped in a controlled manner by atmosphere and ion migration [27–29]. Single-molecule EIS further proves that solvent electrostatics can modulate rectification via interfacial dipole environment [30].

Such a study raises concerns about the stationarity of the measurement. Ions, solvent molecules, and redistribution of charges due to bias can all evolve over time during the frequency sweep. Therefore, a smooth-looking impedance spectrum can mean averaging over a changing state rather than measuring a linear and stationary system. Validation involves a series of repeated measurements, forward and reverse sweeps, tests of bias and history dependence, small signal amplitude checks, relaxation tests, and Kramers–Kronig compliance check. Additionally, nanoseconds time scale ionic motion must be validated separately from parasitic capacitance and instrument bandwidth.

5.4. Protein and bioelectronic junctions

In bioelectronics, proteins form an intriguing category because they raise the question of efficient protein-based conductance versus contact- and interfacial-origin currents. Recent research on molecular junctions constructed from proteins shows that contact modification can significantly change the apparent protein resistance and that EIS can help clarify the origin of currents [31]. The study is important because the regime involves long-range transport, hydration-dependent dielectric response, redox cofactors, and electrode chemistry.

A protein impedance assignment needs length or thickness dependence as a control and contact comparison. If the resistance changes after contact modification and the dependence becomes physically sensible, then the previous contact-limited assignment is supported. Capacitance is to be reported as an effective junction response, reflecting not only the bulk protein response, but also interfacial polarization and charge relaxation. Hydration, molecular conformations, redox state, and electrode chemistry all play a role in capacitance fitting. As a result, biochemical and interfacial state should accompany capacitance assignment.

5.5. Mesoscopic and quantum admittance limit

At mesoscopic dimensions, impedance starts becoming a secondary quantity compared to admittance because quantum RC circuits suggest that capacitance may reflect electron energy levels and charge relaxation [32]. Atomic-scale contacts exhibit vanishingly small reactive admittance up to gigahertz frequencies; therefore, atomic-sized metallic contacts can be regarded almost as resistors with respect to impedance [33–35]. The implication is that when the fitted impedance value exceeds a physically reasonable value for an atomic contact, it is

either parasitic or molecular origin.
The difference between impedance and admittance thus cannot be overlooked because a low imaginary impedance does not imply a low imaginary admittance, and sometimes a different physical picture appears with the switch to admittance. Both $Z(\omega)$ and $Y(\omega)$ should be analyzed for comparative purposes in highly conductive molecular junctions, atomic contacts, and coherent quantum circuits.

6. The Molecular Impedance Credibility Index (MICI)

6.1. Purpose and definition

The MICI translates the validation logic into a parameter-specific measure. The index does not measure the scientific significance of a paper. Rather, it assesses how firmly a specific impedance parameter is validated in a molecular context. The MICI is defined as

$$\mathrm{MICI} = \frac{1}{2N}\sum_{k=1}^{N} s_k, \tag{10}$$

where N is the total number of validation criteria and $s_k \in \{0,1,2\}$ is the score for the k^{th} criterion. A score of 0 means that the criterion is not addressed, 1 implies partial validation, and 2 stands for conclusive validation. Normalization ensures that MICI belongs to $[0,1]$.
A paper should receive a unique MICI for every claimed impedance parameter since some elements can be supported more firmly than others. Even though a paper has a strong contact resistance, its capacitance may lack validation criteria.
Figure 4 demonstrates what MICI is intended to convey: every assigned parameter has a unique evidence profile. A highly supported contact resistance assignment, for example, does not imply validity of CPE-derived capacitance assignment.

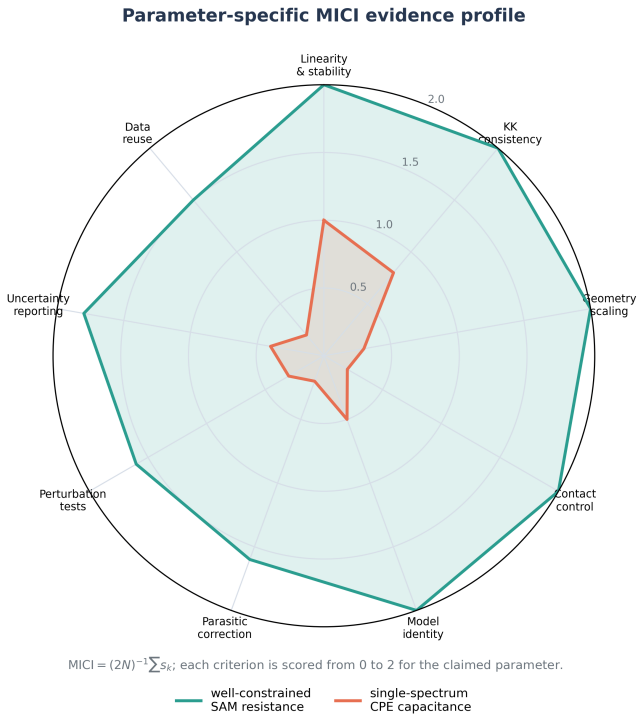

Figure 4: Parameter-specific MICI evidence profile. The scale in the radial direction corresponds to the rubric in Table 3 with criterion scores varying from 0 to 2 and normalization by Eq. (10). The profile illustrates how a molecular resistance can be supported by several criteria, while a capacitance assignment remains less substantiated.

6.2. Interpretation of MICI values

A MICI below 0.35 is a clear indication that a parameter assignment is not credible. Between 0.35 and 0.65 is an intermediate confidence region. Values exceeding 0.65 indicate good evidence for a molecular assignment, provided that the most relevant criteria are addressed. A threshold above 0.80 implies high confidence in molecular assignment and should be reachable in a validation experiment.
The thresholds serve as decision bands for categorizing the confidence in assignment. The MICI score does not imply the absence of any systematic error in the fitting process. On the contrary, the score requires that an analyst state which physical tests, including the perturbation analysis, confirm a molecular assignment.
Claims involving exceptionally high dielectric constants, ultra-fast ionic motion, contact-independent protein conductivity, and quantum molecular admittance all need to be backed up with high MICI scores since the molecular signal has to be distinguished from the instrumental and geometrical ones.

7. Validation-driven interpretation workflow

Figure 5 presents the proposed workflow for interpreting molecular impedance spectra. It includes preliminary validation, inspection, constrained analysis, and parameter assignment and testing. The order of steps is very important since if an experimental spectrum is not linear or stationary, circuit analysis can still provide comparative measures.

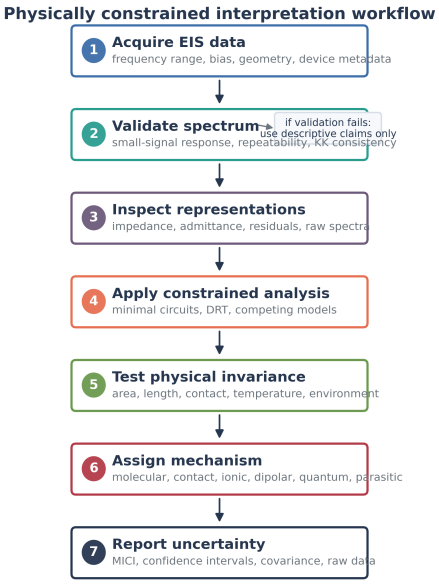

Figure 5: Physically constrained interpretation workflow for molecular and bioelectronic EIS. KK stands for Kramers–Kronig consistency test.

The first step of the process is data documentation. A device area, molecular length, contact architecture, measurement frequency range, AC amplitude, and voltage bias are necessary to compare spectra. The second step is validation. An AC amplitude check is essential because bias can influence molecular conformation, ion concentration, redox equilibrium, and contact properties. The third step is impedance and admittance plotting. The reason is that certain impedances can be interpreted as admittances, especially in high-conductivity or mesoscopic limits.
The next step is constrained analysis. Selection of a physical circuit model precedes parameter assignment, and it requires verification against alternative and competing circuits. DRT analysis can be applied if the device has multiple time constants distributed within a frequency

Table 3: Criteria scores for the Molecular Impedance Credibility Index. The score is assigned to each assignment of an impedance parameter individually.

Criterion	0: Not addressed	1: Partially addressed	2: Convincingly addressed
Linearity and stability	No amplitude or repeatability test	Limited repeat spectra or small signal assumption	Amplitude independence, repeatability, and drift controls reported
Kramers–Kronig consistency	Not reported	Mentioned or visually checked	Quantitative validation and residuals reported
Geometric scaling	Single area or geometry only	Limited area or blank comparison	Scaling consistent with assignment
Contact control	No contact comparison	Contact effect discussed indirectly	Varying contact architecture or control
Model identifiability	Single circuit fit only	Alternative circuits mentioned	Competing models, residuals, and covariance reported
Parasitic correction	No correction or estimate	Discussion of parasitics	Open/short/load, blanks, or layout simulation included
Thermal, bias, environmental	Single condition only	Limited perturbation series	Mechanism-specific perturbation validated
Uncertainty reporting	Point estimates only	Standard deviation reported	Confidence intervals and device statistics
Data reusability	No raw spectra	Figure only or partial data	Raw spectra and fitting code/data available

band. Finally, each parameter is assigned following validation of physical invariance and uncertainty estimation.

Each assignment of a molecular parameter should be based on at least one control that leaves the assigned parameter unchanged and another control that affects it. For instance, a tunneling resistance should depend on length and be insensitive to contact architecture, whereas a molecular capacitance should scale with area inversely to thickness. A capacitive peak due to ionic motion is expected to vary with bias or environment.

8. Parameter assignment safeguards

The interpretation of molecular EIS is robust if the experiment, fitting model, and assignment are all guided by physical constraints. Table 4 lists safeguards that avoid misinterpretation of impedance parameters without limiting the junction architecture.

Table 4: Safeguards against misinterpretation of EIS in molecular junctions.

Assignment challenge	Recommendation
Ambiguous circuit topology	Test against at least one alternative circuit, plot residuals, justify elements physically, and report covariance/confidence intervals.
Ambiguous parasitic contribution	Use short-reference and blank devices, check area and thickness scaling, perform open/short/load tests, and estimate parasitics geometrically.
Overinterpreting CPE behavior	Report fitted CPE parameters and explain the capacitance conversion limits.
Lack of stationarity check	Test for linearity and stability with repeated sweeps, forward/reverse sweeps when possible, and Kramers–Kronig analysis.
Inadequate assignment validation	Check the assigned parameter against length dependence (tunneling), temperature (hopping), contact variation (contact-limited), and environmental conditions (dipolar or ionic).
Low reproducibility of results	Deposit the raw data, code, device statistics, and experimental settings.

The listed safeguards resolve the major challenges that molecular EIS analysis is prone to. Ambiguity of circuit elements can be resolved by performing a test against alternative models and assessing residual structures in addition to parameter assignment. Ambiguity of parasitic contribution can be addressed by using short-reference and blank devices, scaling area and thickness, and checking the geometry. The CPE-based capacitance assignment should always be justified explicitly in terms of a model since otherwise there are no limits to CPE fitting.

The lack of stationarity test should raise a warning flag for EIS because any time evolution of an electrically tunable junction should invalidate the impedance assignment. Assignment of the molecular parameter should be based on a validation against changes that are expected to leave the parameter unchanged or to change it. Uncertainty should be quantified since two fitted parameters with significant covariance cannot be distinguished.

9. Theoretical implications

9.1. From parameter assignment to dynamic molecular transport

In molecular electronics, the most commonly employed parameter descriptors are β, the barrier height, conductance, rectification ratio, and dielectric constant. These parameters provide useful descriptors for molecular electronics; however, molecular impedance allows assigning dynamic transport modes. A molecule can act as a tunneling barrier, as a hopping channel, as a polarizable medium subject to external fields, and even as a medium screening ionic displacement.

The relaxation-time atlas maps these regimes. Tunneling is expected at shorter lengths with stable contacts. Hopping occurs with increased conjugation or redox capabilities. Screening is expected for systems containing charged species, whereas molecular conformation may lead to impedance modulation in a biological junction. At the mesoscopic limit, admittance is preferable since the imaginary part of admittance is a measure of current rather than impedance.

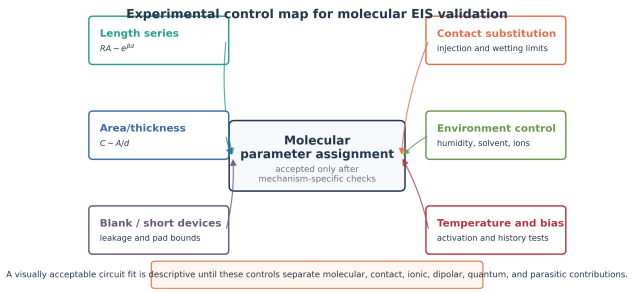

Figure 6: Experimental control map for molecular EIS validation. Molecular parameters require different validation criteria: a length series for a tunneling resistance, an area or thickness dependence for capacitance, blank and short-reference control for parasitics, varying contact architecture for injection barriers, and an environmental control or perturbation protocol for dielectric and ionic mechanisms.

9.2. Effective dielectric constant

One aspect of molecular EIS that is always problematic is the assignment of dielectric constants. Eq. (4) is tempting in the sense that the capacitance can be divided by area to yield the relative permittivity ε_r; however, a junction capacitance is an effective property that includes interfaces, parasitics, and contacts. An apparent dielectric constant should therefore be reported as an effective parameter.

On the contrary, a distinction between a bare molecular parameter and a junction property strengthens the assignment. An anomalously high dielectric constant may stem from a large number of molecules aligned, but equally plausibly the capacitance assignment may involve interfaces, geometrical factors, charge trapping, incomplete parasitics correction, and many other factors.

9.3. From impedance to admittance

Impedance plots are intuitively appealing in the high-resistivity regime since impedance curves are mostly determined by resistance peaks. Impedance is not necessarily the preferred choice when the conductance is relatively high. Admittance is often better since it provides an immediate visualization of the reactive current. Reporting $Z(\omega)$ and $Y(\omega)$ together is therefore recommended when a molecular device operates at high frequencies.

10. Experimental design rules for molecular impedance experiments

The uncertainty atlas implies practical design rules. For molecular resistance, length or thickness dependence is necessary as a control. The area dependence test is needed for capacitance. Control against interfacial parasitics should be provided by blank or short-reference devices. Contact architectures must be changed in order to verify a contact contribution.

Blank and short-reference junctions can serve as controls for leakage and parasitics. Environmental controls must be performed depending on the origin of capacitance: a comparison with vacuum, inert gas, humidity, polar and non-polar solvent, and ion-free conditions allows separating dipolar and ionic capacitance. Measurement history is important, as preconditioning bias, sweeping direction, wait times, solvent immersion, and aging of the junction can impact the measured impedance.

The deposition of raw spectra and data fitting code ensures that impedance analysis is reusable. Experimental datasets must be shared for common junctions, such as SAM junctions, conjugated wires, ion-containing films, protein junctions, atomic contacts, and blanks.

11. Scope and Methodological Limits

MICI and RTA provide practical heuristics rather than a universal theory of molecular impedance. MICI employs semi-quantitative scoring and thus depends on judgment calls. This is acceptable for explicit comparison but cannot replace rigorous uncertainty propagation in the initial fitting stage. Certain experiments, especially single molecule break junctions, might not support area normalization and blank devices, in which case relevant criteria have to be indicated clearly rather than forcing inappropriate scoring.

DRT is inherently model-dependent since it requires regularization and is susceptible to artifacts in a narrow or noisy frequency range. DRT should hence be used to complement circuit fitting, not necessarily to replace it. Retroactive scoring cannot exceed the limitations of the data as provided by the primary article. Thus, older articles might not even contain information about raw spectra, covariance matrices, and validity checks. Derived MICI scores should hence be understood as an assessment of available evidence.

Electrical evidence alone may be insufficient for mechanistic assignment. Additional spectroscopic, microscopic, optical, x-ray, surface chemistry, molecular dynamics, and quantum mechanical data may be needed to distinguish contributions of molecular polarizability, interface chemistry, geometric effects, and the transport mechanism.

12. Research Priorities for Molecular Impedance Metrology

EIS will yield more reproducible results as soon as validation data becomes part of the standard measurement protocol. These data include raw spectra, frequency window, AC amplitude, DC bias, device area, thickness or molecular length, contact design, environment, replicate spectra, and Kramers-Kronig consistency. Publicly available databases need to be compiled for common junction types such as SAM tunnel junctions, conjugated wires, ionic layers, protein films, atomic junctions, and blank devices. Multiscale modeling needs to relate the intrinsic polarizability and electronic interaction of molecules to capacitance, contact resistance, and electric field distributions on the nanoscale.

Time-resolved and operando impedance become increasingly important. Integrating impedance data with optical, Raman, infrared, Kelvin probe, or ultrahigh speed electrical techniques would enable direct distinction of electronic, dipolar, ionic, and structural dynamics beyond the scope of equivalent circuit fitting. This combination is necessary to achieve rigorous tests of ionic motion, rectification tuning, and bioelectronics.

13. Conclusions

EIS will become a quantitative metrology tool for molecular and bioelectronic junctions as long as fitted parameters are linked to physical limits. The RTA provided here categorizes impedance phenomena based on their physical basis, expected scaling, necessity for validation, and risk of improper assignment. The additional MICI parameter assigns a score indicating how much evidence supports the molecular assignment.

The main conclusion is that reliable molecular impedance must agree with respect to geometry, contacts, frequency response, perturbation tests, parasitic compensation, and error estimation. A molecular resistance needs to pass length and contact tests, a capacitance to pass area and thickness tests, an ionic relaxation to pass stationarity and environmental tests, a CPE not to be converted to capacitance without model-based reasoning, and a high-frequency or atomic scale effect to pass admittance tests in addition to impedance.

References

[1] Xiang, D., Wang, X., Jia, C., Lee, T., & Guo, X. (2016). Molecular-scale electronics: From concept to function. *Chemical Reviews*, *116*, 4318–4440.

[2] Jia, C., Lin, Z., Huang, Y., & Duan, X. (2019). Nanowire electronics: From nanoscale to macroscale. *Chemical Reviews*, *119*, 9074–9135.

[3] Li, T., Bandari, V. K., & Schmidt, O. G. (2023). Molecular electronics: Creating and bridging molecular junctions and promoting its commercialization. *Advanced Materials*, *35*, e2209088.

[4] Lacroix, J.-C. (2018). Electrochemistry does the impossible: Robust and reliable large area molecular junctions. *Current Opinion in Electrochemistry*, *7*, 153–160.

[5] Simmons, J. G. (1963). Generalized formula for the electric tunnel effect between similar electrodes separated by a thin insulating film. *Journal of Applied Physics*, *34*, 1793–1803.

[6] Luo, L., Balhorn, L., Vlaisavljevich, B., Ma, D., Gagliardi, L., & Frisbie, C. D. (2014). Hopping transport and rectifying behavior in long donor–acceptor molecular wires. *Journal of Physical Chemistry C*, *118*, 26485–26497.

[7] Taherinia, D., Smith, C. E., Ghosh, S., Odoh, S. O., Balhorn, L., Gagliardi, L., Cramer, C. J., & Frisbie, C. D. (2016). Charge transport in 4 nm molecular wires with interrupted conjugation: Combined experimental and computational evidence for thermally assisted polaron tunneling. *ACS Nano*, *10*, 4372–4383.

[8] Pitie, S., Dappe, Y. J., Maurel, F., Seydou, M., & Lacroix, J.-C. (2024). Marcus theory and long-range activationless transport in molecular junctions. *Journal of Physical Chemistry Letters*, *15*, 6996–7002.

[9] Sangeeth, C. S., Wan, A., & Nijhuis, C. A. (2014). Equivalent circuits of a self-assembled monolayer-based tunnel junction determined by impedance spectroscopy. *Journal of the American Chemical Society*, *136*, 11134–11144.

[10] Sangeeth, C. S., Demissie, A. T., Yuan, L., Wang, T., Frisbie, C. D., & Nijhuis, C. A. (2016). Comparison of DC and AC transport in 1.5–7.5 nm oligophenylene imine molecular wires across two junction platforms: Eutectic Ga–In versus conducting probe atomic force microscope junctions. *Journal of the American Chemical Society*, *138*, 7305–7314.

[11] Chen, X., & Nijhuis, C. A. (2021). The unusual dielectric response of large area molecular tunnel junctions probed with impedance spectroscopy. *Advanced Electronic Materials*, *8*.

[12] Su, M., Ngo, K., Lacroix, J.-C., Turmine, M., & Vivier, V. (2026). EIS measurements in molecular electronics. *Current Opinion in Electrochemistry*, *57*, 101830.

[13] Orazem, M. E., Agarwal, P., & Garcia-Rubio, L. H. (1994). Critical issues associated with interpretation of impedance spectra. *Journal of Electroanalytical Chemistry*, *378*, 51–62.

[14] Vivier, V., & Orazem, M. E. (2022). Impedance analysis of electrochemical systems. *Chemical Reviews*, *122*, 11131–11168.

[15] Gateman, S. M., Gharbi, O., de Melo, H. G., Ngo, K., Turmine, M., & Vivier, V. (2022). On the use of a constant phase element (CPE) in electrochemistry. *Current Opinion in Electrochemistry*, *36*.

[16] Wang, S., Zhang, J., Gharbi, O., Vivier, V., Gao, M., & Orazem, M. E. (2021). Electrochemical impedance spectroscopy. *Nature Reviews Methods Primers*, *1*.

[17] Boukamp, B. A. (1995). A linear Kronig–Kramers transform test for immittance data validation. *Journal of the Electrochemical Society*, *142*, 1885–1894.

[18] Schoenleber, M., Klotz, D., & Ivers-Tiff'ee, E. (2014). A method for improving the robustness of linear Kramers–Kronig validity tests. *Electrochimica Acta*, *131*, 20–27.

[19] Tikhonov, A. N., & Arsenin, V. Y. (1977). *Solutions of ill-posed problems*. Winston.

[20] Weese, J. (1992). A reliable and fast method for the solution of Fredholm integral equations of the first kind based on Tikhonov regularization. *Computer Physics Communications*, *69*, 99–111.

[21] Eckermann, A. L., Feld, D. J., Shaw, J. A., & Meade, T. J. (2010). Electrochemistry of redox-active self-assembled monolayers. *Coordination Chemistry Reviews*, *254*, 1769–1802.

[22] Xing, Y. F., Li, S. F. Y., Lau, A. K. H., & O'Shea, S. J. (2005). Electrochemical impedance spectroscopy study of mixed thiol monolayers on gold. *Journal of Electroanalytical Chemistry*, *583*, 124–132.

[23] Akkerman, H. B., Naber, R. C., Jongbloed, B., van Hal, P. A., Blom, P. W., de Leeuw, D. M., & de Boer, B. (2007). Electron tunneling through alkanedithiol self-assembled monolayers in large-area molecular junctions. *Proceedings of the National Academy of Sciences of the United States of America*, *104*, 11161–11166.

[24] Chen, X., Salim, T., Zhang, Z., Yu, X., Volkova, I., & Nijhuis, C. A. (2020). Large increase in the dielectric constant and partial loss of coherence increases tunneling rates across molecular wires. *ACS Applied Materials & Interfaces*, *12*, 45111–45121.

[25] Heitzer, H. M., Marks, T. J., & Ratner, M. A. (2013). First-principles calculation of dielectric response in molecule-based materials. *Journal of the American Chemical Society*, *135*, 9753–9759.

[26] Hadi, H., Aouled Dlala, N., Cherif, I., Gassoumi, B., Abdelaziz, B., Safari, R., Caccamo, M. T., Magazu, S., Patane, S., Ghalla, H., & Ayachi, S. (2024). Exploring nano-optical molecular switch systems for potential electronic devices: Understanding electric and electronic properties through DFT-QTAIM assembly. *ACS Omega*, *9*, 37702–37715.

[27] Bonifas, A. P., & McCreery, R. L. (2012). Solid state spectroelectrochemistry of redox reactions in polypyrrole/oxide molecular heterojunctions. *Analytical Chemistry*, *84*, 2459–2465.

[28] James, D. D., Bayat, A., Smith, S. R., Lacroix, J. C., & McCreery, R. L. (2018). Nanometric building blocks for robust multifunctional molecular junctions. *Nanoscale Horizons*, *3*, 45–52.

[29] Chandra Mondal, P., Tefashe, U. M., & McCreery, R. L. (2018). Internal electric field modulation in molecular electronic devices by atmosphere and mobile ions. *Journal of the American Chemical Society*, *140*, 7239–7247.

[30] Shi, W., Greenwald, J. E., & Venkataraman, L. (2024). Impact of solvent electrostatic environment on molecular junctions probed via electrochemical impedance spectroscopy. *Nano Letters*, *24*, 9283–9288.

[31] Bera, S., Vilan, A., Das, S., Pecht, I., Ehre, D., Sheves, M., & Cahen, D. (2025). Without contact resistance, proteins in thin-film solid-state junctions can be efficient electronic conducting materials. *Advanced Materials*, e07654.

[32] Gabelli, J., Feve, G., Berroir, J. M., & Placais, B. (2012). A coherent RC circuit. *Reports on Progress in Physics*, *75*, 126504.

[33] Aoyama, S., Kurokawa, S., & Sakai, A. (2015). High-frequency signal transmission through single-atom contacts of Au and Pt. *Applied Physics Letters*, *106*.

[34] Sakai, A. (2018). Admittance of atomic and molecular junctions and their signal transmission. *Micromachines*, *9*.

[35] Hou, J. G., Wang, B., Yang, J., Wang, X. R., Wang, H. Q., Zhu, Q., & Xiao, X. (2001). Nonclassical behavior in the capacitance of a nanojunction. *Physical Review Letters*, *86*, 5321–5324.